Chemical Science

ROYAL SOCIETY OF CHEMISTRY

EDGE ARTICLE

View Article Online
View Journal | View Issue

Cite this: *Chem. Sci.*, 2021, **12**, 2614

All publication charges for this article have been paid for by the Royal Society of Chemistry

Trace mild acid-catalysed $Z \rightarrow E$ isomerization of norbornene-fused stilbene derivatives: intelligent chiral molecular photoswitches with controllable self-recovery†

Taotao Hao,[a] Yongsheng Yang,[a] Wenting Liang,[b] Chunying Fan,[a] Xin Wang,[a] Wanhua Wu,*[a] Xiaochuan Chen,[a] Haiyan Fu,*[a] Hua Chen[a] and Cheng Yang*[a]

Received 21st September 2020
Accepted 28th December 2020

DOI: 10.1039/d0sc05213b

rsc.li/chemical-science

Stilbene derivatives have long been known to undergo "acid-catalyzed" $Z \rightarrow E$ isomerization, where a strong mineral acid at high concentration is practically necessary. Such severe reaction conditions often cause undesired by-reactions and limit their potential application. Herein, we present a trace mild acid-catalyzed $Z \rightarrow E$ isomerization found with stilbene derivatives fused with a norbornene moiety. By-reactions, such as the migration of the C=C double bond and electrophilic addition reactions, were completely inhibited because of the ring strain caused by the fused norbornene component. Direct photolysis of the E isomers at selected wavelengths led to the $E \rightarrow Z$ photoisomerization of these stilbene derivatives and thus constituted a unique class of molecular switches orthogonally controllable by light and acid. The catalytic amount of acid could be readily removed, and the $Z \rightarrow E$ isomerization could be controlled by turning on/off the irradiation of a photoacid, which allowed repeated isomerization in a non-invasive manner. Moreover, the Z isomer produced by photoisomerization could spontaneously self-recover to the E isomer in the presence of a catalytic amount of acid. The kinetics of $Z \rightarrow E$ isomerization were adjustable by manipulating catalytic factors and, therefore, unprecedented molecular photoswitches with adjustable self-recovery were realized.

Introduction

The Z–E isomerization of stilbene derivatives has been known for over one century,[1] and it has now become one of the most representative prototype reactions applied to molecular machines,[2] such as molecular motors,[3] photoswitches,[4] molecular ratchets[5] and half adders,[6] mainly due to the significant geometrical changes that occur during reversible isomerization. The Z–E isomerization of stilbene derivatives has been extensively investigated and is currently known to be triggered by physical (light or temperature) or chemical activators, such as boron fluoride-ether complexes,[7] acids[8] and bromine, in conjunction with light.[9] Photoisomerization is most commonly applied in molecular machines due to its non-invasive and convenient operating features.[10]

On the other hand, protic acids have long been known to promote the $Z \rightarrow E$ isomerization of stilbene derivatives *via* an A-SE2 mechanism.[11] However, such acid-catalysed isomerization commonly requires the use of strong mineral acids at high concentrations as the solvent, which significantly limits the application of this method due to low functional group tolerance and undesired side reactions caused by the harsh reaction conditions.[12] The use of a large excess of strong acids is particularly unfavourable for molecular machines in terms of non-accumulative repeating operations. For an ideal chemically activated molecular machine, the chemical inductor should be mild, work in a catalytic amount, and be readily removable/deactivated.[13] To our knowledge, such molecular machines based on stilbene derivatives have not yet been documented.

Although stimulus-responsive molecular switches have been widely constructed based on chemical and physical stimuli, including light,[14] electrochemistry,[15] temperature,[16] pH,[17] solvent,[18] and additives,[19] and we have established rotating switches consisting of molecular universal joints based on thermal[20] and redox stimuli,[21] the molecule switches obtained by such sophisticated design and synthesis are generally responsive to only one of the above stimuli, and few molecular switches can be manipulated by two independent effectors,[2a,f,13] which would offer a higher level of

[a]*Key Laboratory of Green Chemistry & Technology, College of Chemistry, Sichuan University, 29 Wangjiang Road, Chengdu 610064, China. E-mail: yangchengyc@scu.edu.cn*

[b]*Institute of Environmental Science, Department of Chemistry, Shanxi University, Taiyuan 030006, China*

† Electronic supplementary information (ESI) available. CCDC **5Z**: 1949916, **5E1**/**5E2**: 1949886 and **6E**: 1949917. For ESI and crystallographic data in CIF or other electronic format see DOI: 10.1039/d0sc05213b

control.[22] Herein, we report $Z \rightarrow E$ isomerization of a novel kind of stilbene derivative unprecedentedly catalysed by even a trace amount of a mild organic acid. Double control of the *Z–E* isomerization by the two independent external stimuli of light and acid, so-called orthotropic control,[22a] was realized (Fig. 1a), resulting in intriguing and advanced functions in these molecular photoswitches. The unique self-recovery behavior has been widely presented in nature, *e.g. Nymphaea tetragona*, which self-recover between OFF (night) and ON (day) with light and chemical stimuli (Fig. 1c). Hence, the overall dynamic properties of the newly prepared stilbene derivative switches mimicked the behaviors of the macroscopic *Nymphaea tetragona* well.

Results and discussion

Z-to-*E* isomerization of norbornene-fused stilbene derivatives catalysed by a trace amount of mild acid

The present study was essentially prompted by a casual observation of spontaneous chemical conversion of **5Z** (Fig. 1), which was synthesized by a one-pot stereoselective Pd-catalysed domino reaction (Scheme S6†).[23] As illustrated in Fig. 2, a new set of proton signals separate from the original signals of **5Z** appeared during the ^{1}H NMR spectral measurements of **5Z** in $CDCl_3$ (Fig. 2a and b). This chemical conversion progressed smoothly over time even under strict light-proof conditions, which is unexpected because both the *Z* and *E* forms of stilbene derivatives are, in general, thermally stable. This observation prompted us to perform further NMR investigations in different deuterated solvents. Indeed, **5Z** has excellent thermal stability, and no chemical conversion was observed in the ^{1}H NMR spectra by heating **5Z** in DMSO-d_6 at 130 °C for over 24 h (Fig. 2d and e). Further NMR experiments revealed that spontaneous chemical conversion could be observed only in newly opened $CDCl_3$ but not in other deuterated solvents. To examine the possible effects of oxygen, we deoxygenated the solutions by bubbling nitrogen into the $CDCl_3$ solution, which inhibited the reaction. Surprisingly, bubbling oxygen did not facilitate the chemical conversion but instead inhibited it (Fig. S41m†); therefore, we speculated that removal of volatile gas dissolved in $CDCl_3$ by bubbling either N_2 or O_2 should be responsible.

The newly formed compound was then isolated and characterized as the *E* isomer **5E** on the basis of HR mass and 2D NMR spectroscopic studies (Fig. S15–S18†). We then considered that the tiny amount of DCl due to the photodecomposition of $CDCl_3$ may play a role in the spontaneous isomerization of **5Z**. To confirm this hypothesis, we added a drop of aqueous DCl to the $CDCl_3$ solution of **5Z** at room temperature and observed that isomerization rapidly produced **5E** in quantitative yield, as determined by monitoring the ^{1}H NMR spectral changes.

Alkenes are known to undergo electrophilic addition with mineral acids.[24] Alternatively, (*Z*)-stilbene derivatives, mediated by a strong mineral acid,[8] isomerize to the *E* isomers, where proton transfer to the C=C double bond is the rate-determining step. The latter was defined as acid-catalysed isomerization, even though a large excess (commonly >50 wt%) of the strong mineral acids was generally required. The above observation is

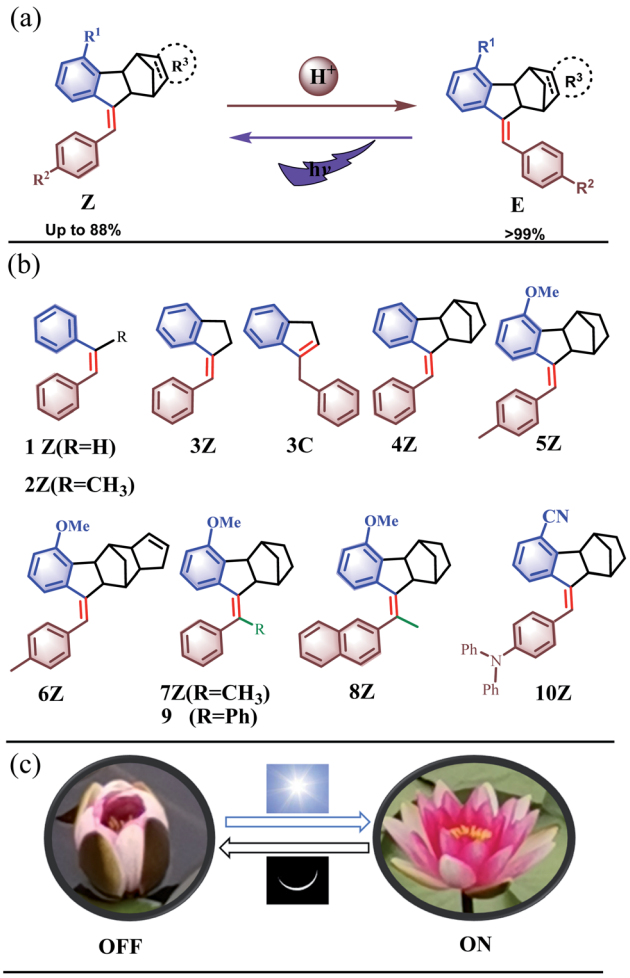

Fig. 1 (a) Orthotropic control of the *Z–E* isomerization of norbornene-fused stilbene derivatives by acid and light, (b) the chemical structure of the stilbene derivatives, and (c) schematic representation of the self-recovery process. The overall dynamic properties of the norbornene-fused stilbene derivative switches mimic those of the macroscopic *Nymphaea tetragona*, which self-recover between OFF (night) and ON (day) under light and chemical stimuli.

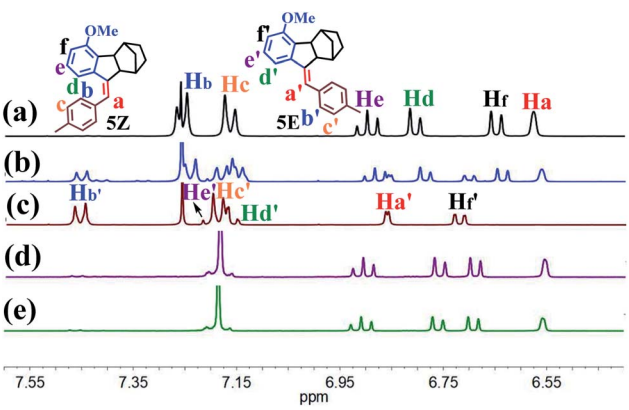

Fig. 2 ^{1}H NMR spectra of **5Z** (a) in $CDCl_3$ sealed with K_2CO_3, (b) in newly opened $CDCl_3$ (which contains a tiny amount of acid), (c) with addition of 0.5 eq. of TFA to $CDCl_3$, (d) in DMSO-d_6 measured soon after preparing the solution, and (e) in DMSO-d_6 after heating at 130 °C for 24 h. All measurements were performed at room temperature.

thus unprecedented and prompted us to test the catalytic effect of different kinds of acids. The isomerization of **5Z** occurred smoothly in the presence of 0.5 eq. of mineral acid, including HCl, HBr and H_2SO_4. Surprisingly, when a milder, organic acid, trifluoroacetic acid (TFA), was used instead of DCl to $CDCl_3$, **5Z** also underwent isomerization to give **5E** within 30 min (Fig. 2c). Catalytic isomerization could be accomplished in the presence of 1% eq. of TFA by increasing the reaction time (Table S1†). The isomerization also proceeded smoothly in the presence of a weaker organic acid, including difluoroacetic acid and dichloroacetic acid.

To understand this exceptional phenomenon, we synthesized a series of stilbene derivatives **4–10** (Fig. 1b) through a reported method,[23] the possible absolute configurations of which are shown in Scheme S6,† and we further examined their proton-catalysed isomerization behaviour. The addition of an equal amount of TFA to the $CDCl_3$ solution of **1Z** did not cause any isomerization even after standing at room temperature for 1 week (Fig. S37c†). The same was true with **2Z** (Fig. S38c†). However, the addition of TFA to the solution of **3Z** not only afforded $Z \rightarrow E$ isomerization product **3E** but also led to migration of the C=C double bond to give endocyclic alkene **3C**. A **3E** : **3C** ratio of 37 : 63 was finally achieved when equilibrium was reached after four days (Fig. S39e†). In contrast, **4Z–6Z** gave the *E* isomers in quantitative yield under the catalysis of TFA (Fig. S40–S44†), demonstrating a unique chemical reaction behaviour due to the introduction of the norbornene moiety.

The mechanism of proton-catalysed isomerization and quantitative *Z*-to-*E* conversion

To gain insight into the mechanism of such unprecedented proton-catalysed isomerization, we monitored the ^{1}H-NMR spectral change of **5Z** in the presence of DCl. As illustrated in Fig. 3b, the addition of DCl into the $CDCl_3$ solution of **5Z** afforded **5E** quantitatively within 2 h to give a relative integration of H_a' of 0.35 (Fig. 3a and b), demonstrating that the proton was partially deuterated. On the other hand, the addition of DCl to the $CDCl_3$ solution of **5E** did not yield any **5Z**, but the integrated intensity of H_a' also decreased with time (Fig. S41†), indicating that the H_a' proton of **5E** was also exchanged by deuterium. These results implied that both *Z* and *E* isomers experienced a carbenium ion intermediate formed by proton transfer. Interestingly, when excess DCl (20 eq.) was added to **5Z**, the protons H_d' and H_f' were also replaced by deuterium at approximately 82% after 48 h (Fig. 3c–f). Based on these observations, we propose that the proton-catalysed isomerization of **5Z** is accomplished through the process shown in Scheme S10.† Thus, D^+ transfers to the C=C double bond of **5Z** first to give intermediate **5I**. Carbenium ion **5I** is then inverted to the relatively stable species **5II**. Elimination of H_a or D from **5II** leads to the *E* isomer. Further deuterium experiments indicated that the deuteration of H_d' and H_f' is a slow process and that H_d' and H_f' can be completely replaced by D only in the presence of a large excess of DCl.

A comparison between **5Z** and **3Z** enabled us to better understand the role of the norbornene moiety. Surprisingly,

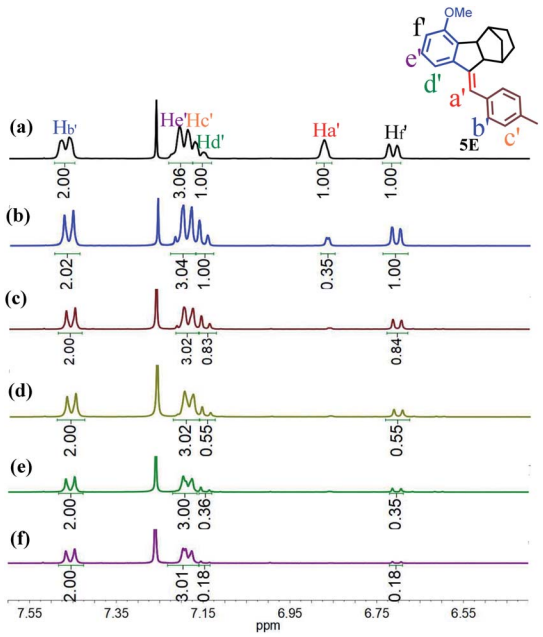

Fig. 3 (a) ^{1}H NMR spectra of **5E** in $CDCl_3$, (b) ^{1}H NMR spectra of the solution after the addition of 2.0 eq. of DCl to the solution of **5Z** in $CDCl_3$ for 2 h, and (c–f) ^{1}H NMR spectra of the solution after the addition of 20 eq. of DCl to the solution of **5Z** in $CDCl_3$ for (c) 2 h, (d) 16 h, (e) 24 h, and (f) 48 h.

freshly prepared **3Z** spontaneously isomerized even in the absence of an acid to give endocyclic alkene **3C** and **3E**, and a **3C**/**3E** ratio of 89 : 11 was achieved after six days (Fig. S39c†). In contrast, all norbornene-fused stilbenes **4Z–10Z** were stable and did not show spontaneous migration of the C=C double bond or isomerization in solution. Even in pure TFA, **5Z** led to **5E** only, and no formation of **5C** or other by-products was observable (Fig. S41k†), which was attributed to the intense ring strain[25] in **5C** due to the fused norbornene moiety. In contrast, **1Z** and **3Z** produced complicated unknown products in TFA (Fig. S37e and S39f†).

The quantitative conversion of **5Z** to **5E** under proton-catalysis conditions was slightly unexpected; in particular, the much larger fused norbornene moiety was expected to cause greater steric repulsion upon rotation of the benzene ring to the norbornene side in the *E* isomer. To clarify this finding, we grew single crystals of both **5Z** and **5E** and carefully analysed the corresponding bond and angle parameters through X-ray single-crystal studies (Fig. 4). The α angle (130.53°) of **5Z** was larger than the β angle (128.12°) of **5E**, implying a smaller steric repulsion caused by the norbornene side than the benzene side.

The dihedral angles θ between the methoxybenzene plane (blue) and the methylbenzene plane (red) were 56.15° for **5Z** and 36.48° for **5E** (Fig. 4b and e), which clearly indicated that the *E* isomer had better coplanarity and therefore more effective conjugation than the *Z* isomer.

Moreover, detailed analyses of the single crystal of **5E** revealed that the norbornene moiety leans to one side of the ring. H18 deviated from the C=C plane (orange) at a distance of 1.613 Å (Fig. 4f). In contrast, the H4 proton on the

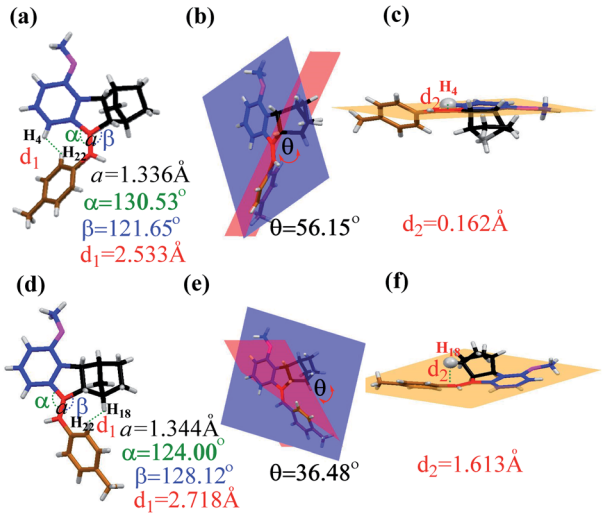

Fig. 4 Single-crystal structures of **5Z** and **5E** (thermal ellipsoid plots at the 50% probability level). The structural parameters for **5Z** (a–c) and **5E** (d–f).

methoxybenzene ring lies almost completely in the plane, which unavoidably causes strong steric interaction with the methylbenzene ring with *cis* configuration (Fig. 4c). These results accounted for the extremely high $Z \rightarrow E$ conversion in these norbornene-fused stilbenes. Similar differences could be found by comparison of the corresponding parameters obtained from the single-crystal structures of **6Z** and **6E** (Fig. S49, Table S2†).

On the other hand, **7Z** and **8Z**, in which the alkylene proton was replaced by a methyl group, also underwent isomerization in the presence of TFA but gave the *E* isomers in 52% and 10% yields, respectively, when equilibrium was reached (Fig. S45 and S46†). The lower *E*/*Z* ratio for the isomerization of **7Z** and **8Z** could be ascribed to the stronger steric repulsion between the methyl group and the methoxy benzene ring in the *E* isomer, which makes the *E*-type carbocation much less stable.

Theoretical study of the proton-catalysed reaction

Styrene is known to undergo an addition reaction with TFA.[26] However, no addition products could be detected with the norbornene-fused stilbene derivatives (Fig. S40–48 and S96†). To understand this interesting phenomenon, two possible reaction routes were compared based on density functional theory (DFT) calculations. The computational simulation suggested that **4Z** and TFA formed an activated complex **com_4Z**, which led to the transition state **TS-4Z-TFA** and then the intermediates **4Z-INT**. The bond rotation of **4Z-INT** gave **4E-INT-1** and **4E-INT-2**, which pass through the transition states **TS-4E-TFA** and **TS-4C-TFA**, respectively, to finally give **4C** and **4E** (Fig. 5). The calculations demonstrated that the Gibbs free energy of **4Z** is higher by 2.7 kcal mol^{-1} than that of **4E** but is lower by 9.0 kcal mol^{-1} than that of **4C**, which is entirely consistent with the results of quantitative conversion to **4E** under acid catalysis.

In particular, **TS-4C-TFA** showed an extremely high Gibbs energy of 30.5 kcal mol^{-1}, further supporting the complete inhibition of the migration of the C=C double bond pathway. On the other hand, **3C** showed a Gibbs energy lower than that of **3Z** by −5.0 kcal mol^{-1} and lower than that of **3E** by −3.1 kcal mol^{-1} (Fig. S97†), agreeing well with the high ratio of the endocyclic alkene product obtained with **3Z**. Thus, the presence of a fused norbornene significantly increased the energy of both **4C** and the intermediates affording **4C** and hence completely impeded the migration of the C=C double bond route. On the other hand, the Gibbs energies of the rate-determining step to the transition state (**TS-1Z-TFA** *vs.* **TS-3Z-**

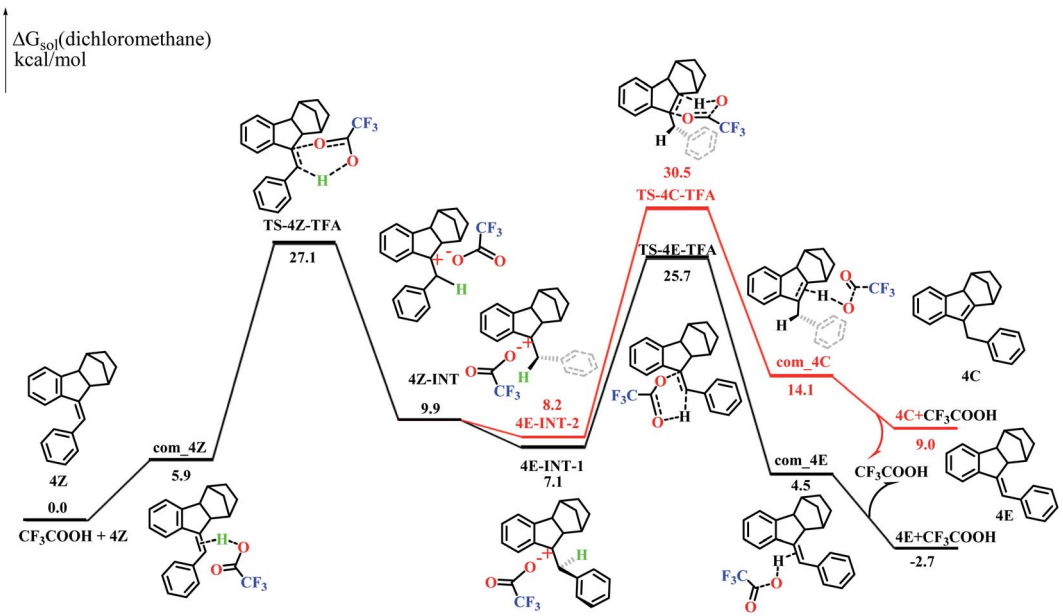

Fig. 5 Calculated energy profiles of 4Z to 4E and 4C.

TFA) in the **1Z** and **3Z** pathways were 41.5 kcal mol^{-1} and 26.5 kcal mol^{-1} (Fig. S97†), respectively. The more conjugation of the benzene ring with vinyl in **3Z**[1d] as well as the tension[25] resulting from the fusion of five-membered rings should be responsible for the much lower Gibbs energies, and this accounted for the lack of observation of isomerization of **1Z** under mild acid conditions.

Factors influencing the proton-catalysed isomerization and non-accumulative cycles

The rate of the proton-catalysed isomerization process was clearly influenced by the solvents used. For example, the isomerization was completed within 2 h in DCM and $CHCl_3$ in the presence of 0.5 eq. of TFA (Table S1, Fig. S67†) but required a longer time in *n*-hexane and toluene and several days in CH_3CN. However, when THF, MeOH, EtOH, or 1,4-dioxane was used as the solvent, no isomerization could be observed, even after 72 h, which was attributed to the stronger solvation of protons in these polar solvents.[27]

The UV-vis spectra of the *Z* and *E* isomers of these norbornene-fused stilbene derivatives are distinctively different, and the isomerization could be conventionally detected from UV-vis spectral changes. As illustrated in Fig. 6a, **5Z** exhibited one broad absorption band that peaked at λ_{max} = 298 nm. The addition of TFA to the solution of **5Z** in DCM led to an apparent increase in absorption to finally give three clear vibrational bands with peaks at 307, 321, and 337 nm, with two isosbestic points (Fig. S64†). It should be noted that, as a very diluted substrate **5Z** is required for UV-vis detection, we used superstoichiometric TFA to accelerate the isomerization. However, a catalytic amount of TFA could indeed lead to quantitative isomerization of **5Z** at high concentrations as can be seen in Fig. 2c, S41, S92 and Table S1.† The isomerization rate increased with the amount of acid, and the extent of $Z \rightarrow E$ conversion could be finely manipulated by controlling the amount of acid and the reaction time. In the presence of a large amount of TFA, isomerization was completed within a few seconds (Fig. 6b). The acid-catalysed isomerization proceeded smoothly even at temperatures as low as −40 °C (Fig. S69†). The isomerization rate could be finely tuned by varying the temperature, and increasing the temperature led to an increase in the reaction rate (Fig. S68†). By manipulating the above

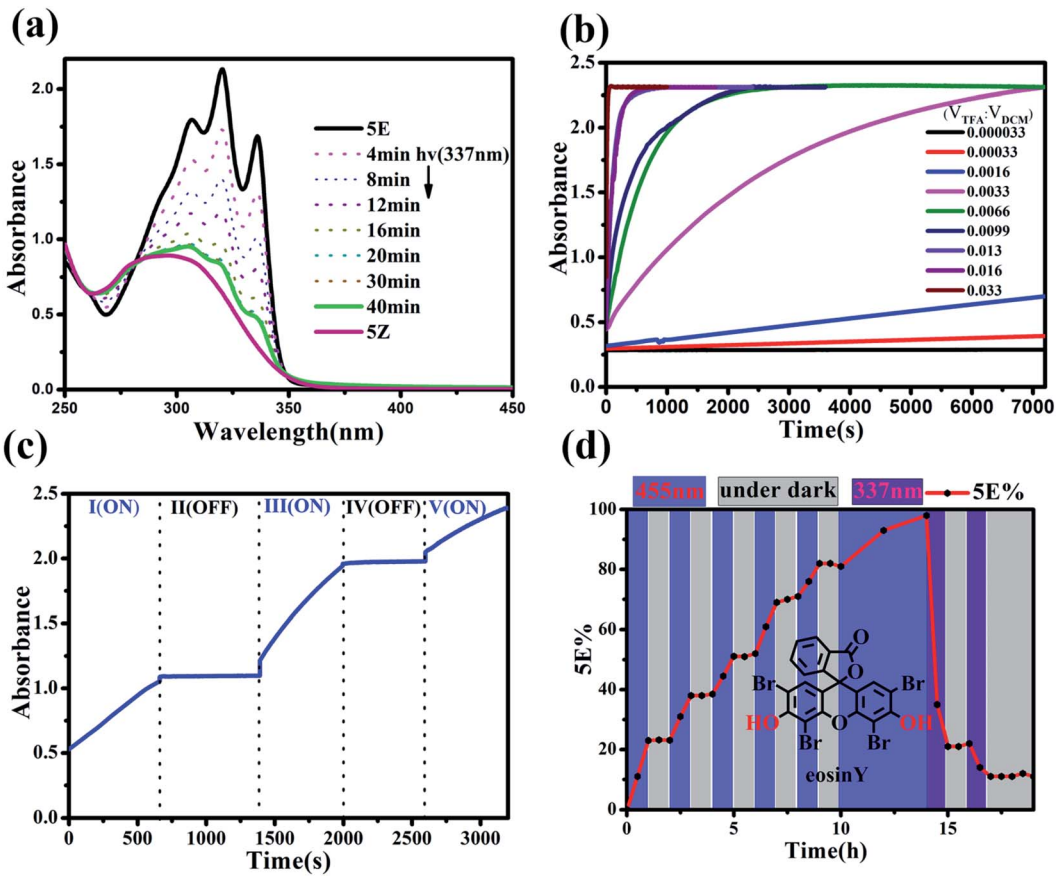

Fig. 6 (a) Changes in the UV-vis spectra of **5E** (5×10^{-5} M in DCM) upon 337 nm UV irradiation for different time periods, (b) changes in time for the absorbance at 337 nm after the addition of different amounts of TFA to the solution of **5Z** (1×10^{-4} M in DCM), and (c) control of the isomerization rate of **5Z** by the addition of TFA and Et_3N. Conditions: stage I: addition of TFA (V_{TFA} : V_{DCM} = 0.0033); stage II: addition of Et_3N; stage III: addition of TFA (V_{TFA} : V_{DCM} = 0.0066); stage IV: addition of Et_3N; stage V: addition of TFA (V_{TFA} : V_{DCM} = 0.0099). (d) Changes in the proportion of **5E** with eosin Y as the photoacid catalyst (0.1 mmol **5Z** and 0.008 mmol eosin Y in 3.0 ml DCM) and the proportion of **5E** determined by HPLC analysis.

factors, the isomerization rate could be flexibly tuned from seconds to days.

Seminal pH-activated *Z*–*E* switches based on the isomerization of hydrazone[28] or enamine[29] have recently been explored by using a protic acid as the hydrogen bonding regulator, in which the acid acted as a reactant and the reverse process required the addition of a base to neutralize the acid, which unavoidably led to the generation of waste and side products that eventually hindered the cycle process.[30] In the present system, isomerization could be accomplished in the presence of only a catalytic amount of protic acid, which allowed stopping the $Z \rightarrow E$ isomerization by adding a small amount of alkali. As illustrated in Fig. 6c, the $Z \rightarrow E$ isomerization of **5Z** can be switched on/off by adding TFA and Et_3N sequentially. On the other hand, the TFA or HCl could be easily removed from the solution simply by bubbling with nitrogen (Fig. S94 and S95†), thus avoiding the accumulative contamination commonly suffered in chemically induced reversible processes.

Moreover, catalytic isomerization by mild acids allowed another alternative for non-invasive control by the use of a photoacid. The $Z \rightarrow E$ isomerization of **5Z** was examined in the presence of 8% eq. of a commercial photoacid, eosin Y, which releases protons upon photolysis but returns to a neutral species in the dark.[31] Indeed, **5Z** underwent $Z \rightarrow E$ isomerization when the system was photoirradiated with a 455 nm OLED, and the isomerization could be stopped by simply turning off the light (Fig. 6d and S91–S93†).

Molecular switch orthogonally controlled by light and acid

The much stronger absorption of **5E** in the long-wavelength range is consistent with the better conjugation properties of **5E**, and $E \rightarrow Z$ photoisomerization could be performed by selective excitation at the absorption peak of **5E**. As shown in Fig. 6a, when **5E** was irradiated with 337 nm UV light in DCM, spectral changes opposite to those of the acid-catalysed isomerization (Fig. S64†) were observed. No further absorption change could be seen after irradiation for 30 min, and a photostationary state (PSS) ratio of **5Z** : **5E** = 88 : 12 was determined by HPLC analysis. These results revealed that the $Z \rightarrow E$ and $E \rightarrow Z$ isomerization of these norbornene-fused stilbenes could be independently manipulated by acid and light, which makes them highly unique molecular switches capable of orthogonal control.[22]

This orthogonal control makes these molecular switches promising for accomplishing complex functions. For example, they can be used as intelligent molecular switches with controllable self-recovery. Self-recovery switches have wide applications from everyday illumination to microcirculation and are critical in computers and accessory protection.[32] A crucial issue for self-recovery switches lies in the precise control of the recovery timescale. The *E*-to-*Z* photoisomerization kinetics of the present system can be conveniently controlled by the irradiation light power. Even in the presence of a certain amount of TFA, the $E \rightarrow Z$ photoisomerization of **5E** proceeded smoothly under intensive irradiation, and turning off the light led to spontaneous $Z \rightarrow E$ isomerization. Without the addition of any base, the on/off switching cycle could be repeated more than 25 times (Fig. S70–S72†). Notably, certain *Z* forms of molecular switches, such as azobenzene derivatives, can thermally isomerize to the *E* form, but the thermal isomerization kinetics primarily depend on the inherent molecular properties and are difficult to manipulate.[33] In contrast, both the $Z \rightarrow E$ and $E \rightarrow Z$ isomerization kinetics of the present molecular switch system are finely controllable. As exemplified in Fig. 7, by changing the concentration of TFA, the recovery time could be conveniently manipulated in a wide time range and therefore should significantly improve the application scenarios of self-recovery.

The potential functional group tolerance was further investigated considering the mild catalysis conditions of the present $Z \rightarrow E$ isomerization system. For example, compound **10Z**, which bears an electron-donating diphenylamino group and an electron-withdrawing cyano group, underwent isomerization smoothly under acid-catalysis conditions. The electronic push–pull effect extends the absorption of **10Z** to the visible range, showing an absorption peak at 400 nm, which is a 102 nm bathochromic shift compared with the parent molecule **4Z** (Fig. S59†). A blue fluorescence emission was observed for **10Z** upon excitation at 380 nm. Upon the addition of TFA to **10Z** in DCM, the UV/vis and PL (photoluminescence) spectra showed obvious changes to finally give **10E** exclusively (Fig. S87 and S88†). The interconversion between **10E** and **10Z** could be conducted by acid and visible light for multiple cycles without any loss in performance. The tolerance of additional functional groups, such as **6Z** and **10Z**, makes it possible to extend the application of this series of compounds through further derivatization or functionalization.

Chiral molecular switch

Norbornene-fused stilbene derivatives are inherently chiral, bearing four stereogenic centers (C7, C8, C11, and C12) in the

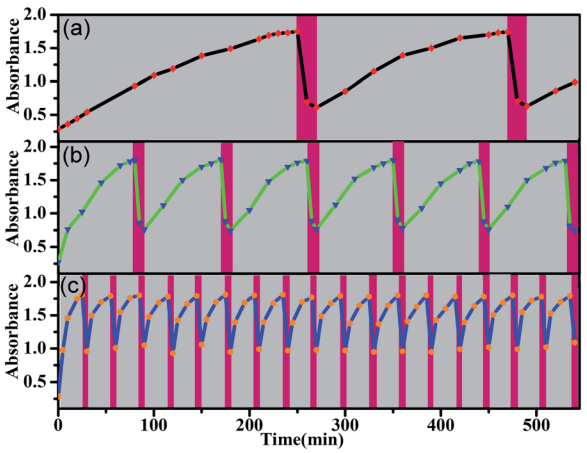

Fig. 7 Photoisomerization and recovery cycles of **5Z** (5×10^{-5} M in DCM) in the presence of TFA (V_{TFA} : V_{DCM}) (a) 0.0016, (b) 0.0033 and (c) 0.0066 at room temperature. The red and grey areas represent photoisomerization (with 337 nm UV irradiation) and self-recovery processes, respectively.

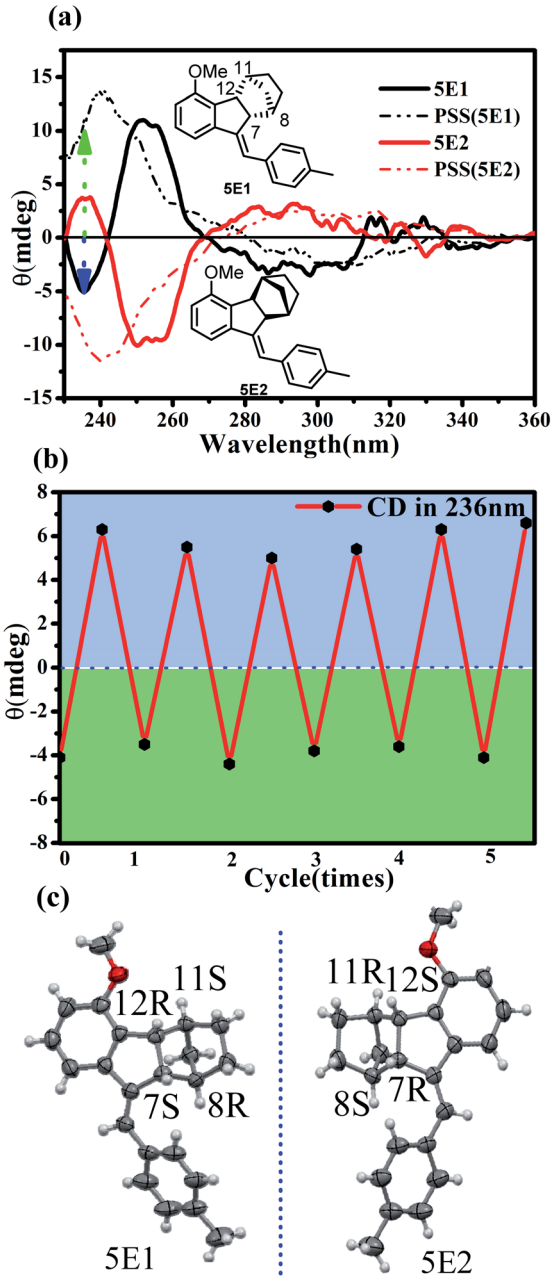

Fig. 8 (a) CD spectral changes of **5E1** and **5E2** (5×10^{-5} M) in *n*-hexane upon irradiation with 337 nm UV light. (b) CD intensity changes at 236 nm for **5E1** (5×10^{-5} M in *n*-hexane) in the presence of TFA ($V_{TFA} : V_{n\text{-hexane}} = 0.0066$) after irradiation with 337 nm and then turning off the light until recovery for five cycles. (c) Single-crystal structures of **5E1** and **5E2** (thermal ellipsoid plots at the 50% probability level).

norbornene component. Our previous studies demonstrated that photochirogenesis is a powerful tool for reading and sensing the supramolecular arrangement of photosubstrates.[34] Compared to conventional photochromic systems, chiral molecular switches provide the unique advantage of non-destructive read-out by detecting optical rotation.[35] The enantiomeric resolution of **5E** was successfully achieved by chiral HPLC (IA column, Fig. S91b†) using a mixed solvent system of *n*-hexane and DCM ($V_{n\text{-hexane}} : V_{DCM} = 80 : 20$). The first eluted fraction **5E1** and the second eluted fraction **5E2** showed perfect mirror-image circular dichroism (CD) spectra, demonstrating an enantiomeric relationship (Fig. 8a). Single crystals of both **5E1** and **5E2** were successfully grown, and the X-ray diffraction analyses demonstrated that the absolute configurations of **5E1** and **5E2** were (7*S*,8*R*,11*S*,12*R*) and (7*R*,8*S*,11*R*,12*S*) (Fig. 8c), respectively. The CD spectrum of **5E1** showed clear negative peaks at 236 nm and 300 nm and a positive peak at 252 nm. Irradiation of enantiopure **5E1** at 337 nm led to apparent CD spectral changes (Fig. 8a).

In particular, in the short wavelength region of 230–245 nm, signal inversion from positive to negative was observed. The original negative peak at 236 nm was sharply inverted to a positive peak. This makes it possible to detect *E*/*Z* or on/off switching on the basis of the CD sign rather than the spectral intensity of common molecular switches. As illustrated in Fig. 8b, alternately turning on and off the photoirradiation led to switching of the CD signal at 236 nm between −4 and +6, offering an unambiguous on/off signal read-out of the molecular switch. On the other hand, optical rotation measurements indicated that (7*R*,8*S*,11*R*,12*S*)-**5E2** has a specific rotation of 119 deg cm^3 dm^{-1} g^{-1} at 20 °C with the sodium D line (589 nm) that drastically changed to 226 deg cm^3 dm^{-1} g^{-1} in the PSS under photoirradiation at 337 nm but completely recovered after adding TFA. Therefore, non-destructive read-out of the switching state of **5** could thus be realized by detecting the specific rotation changes.

Conclusions

In summary, we demonstrated an unprecedented catalytic *Z*-to-*E* isomerization of the C=C bond in a novel kind of norbornene-fused stilbene derivative triggered by a trace amount of mild organic acids, which is in sharp contrast to the concentrated strong mineral acids required in conventional acid-catalysed isomerization of stilbenes. Such mild catalysis of *Z*-to-*E* isomerization occurred quantitatively without any electrophilic addition or migration of the C=C double bond by-reaction. The unique properties of these stilbene derivatives make them promising as a novel kind of molecular switch that has the following advantages: the kinetics of $Z \rightarrow E$ isomerization could be controlled well by the acidity and concentration of acids, temperature and solvents. Photoirradiation at a selected wavelength led to $E \rightarrow Z$ isomerization in excellent conversion to realize the first molecular switches that are orthogonally manipulated by acid and light, respectively. The $Z \rightarrow E$ isomerization could be stopped without contamination by using photoacids or removing the acid by bubbling, and therefore, the acid-catalysed $Z \rightarrow E$ and photo-induced $E \rightarrow Z$ isomerization switching process could proceed through multiple cycles in a non-accumulative fashion. Molecular switches with controllable self-recovery were thus realized based on these excellent properties. Theoretical studies indicate that the ring strain of the norbornene-fused five-membered ring formed upon stilbene conjugation reduces the activation energy of proton transfer and prevents C=C migration, which is

responsible for the unprecedented catalysis of isomerization. We believe that similar properties should be achievable through reasonable chemical modification of the fused ring of stilbene, thus opening a new avenue for stilbene derivatives with highly complex functions.

Conflicts of interest

There are no conflicts to declare.

Acknowledgements

We acknowledge the support of this work by the National Natural Science Foundation of China (No. 21871194, 92056116, 21971169, 21572142 and 22072099), the National Key Research and Development Program of China (No. 2017YFA0505903), the Science & Technology Department of Sichuan Province (2019YJ0160, 2019YJ0090, and 2017SZ0021), and the Fundamental Research Funds for the Central Universities (20826041D4117). Compound characterization was performed with the support of the Comprehensive Training Platform of Specialized Laboratory, College of Chemistry and Professor Peng Wu of the Analytical & Testing Center, Sichuan University.

Notes and references

1 (*a*) J. Wislicenus and M. Jahrmarkt, *Chem. Zentralbl.*, 1901, **I**, 463; (*b*) J. Saltiel, S. Gupta, D. W. Eaker, A. M. Kropp and V. K. R. Kumar, *Photochem. Photobiol.*, 2018, **94**, 247; (*c*) W. Fuß, C. Kosmidis, W. E. Schmid and S. A. Trushin, *Angew. Chem., Int. Ed.*, 2004, **43**, 4178; (*d*) J.-S. Yang, C.-K. Lin, A. M. Lahoti, C.-K. Tseng, Y.-H. Liu, G.-H. Lee and S.-M. Peng, *J. Phys. Chem. A*, 2009, **113**, 4868.

2 (*a*) S. Erbas-Cakmak, D. A. Leigh, C. T. McTernan and A. L. Nussbaumer, *Chem. Rev.*, 2015, **115**, 10081; (*b*) I. Tochitsky, M. A. Kienzler, E. Isacoff and R. H. Kramer, *Chem. Rev.*, 2018, **118**, 10748; (*c*) M. Irie, T. Fukaminato, K. Matsuda and S. Kobatake, *Chem. Rev.*, 2014, **114**, 12174; (*d*) E. R. Kay, D. A. Leigh and F. Zerbetto, *Angew. Chem., Int. Ed.*, 2007, **46**, 72; (*e*) D. Dattler, G. Fuks, J. Heiser, E. Moulin, A. Perrot, X. Yao and N. Giuseppone, *Chem. Rev.*, 2020, **120**, 310; (*f*) M. Baroncini, S. Silvi and A. Credi, *Chem. Rev.*, 2020, **120**, 200; (*g*) A. W. Heard and S. M. Goldup, *ACS Cent. Sci.*, 2020, **6**, 117.

3 (*a*) N. Koumura, R. W. J. Zijlstra, R. A. van Delden, N. Harada and B. L. Feringa, *Nature*, 1999, **401**, 152; (*b*) B. L. Feringa, *Angew. Chem., Int. Ed.*, 2017, **56**, 11060; (*c*) V. García-López, D. Liu and J. M. Tour, *Chem. Rev.*, 2020, **120**, 79.

4 (*a*) J.-F. Xu, Y.-Z. Chen, D. Wu, L.-Z. Wu, C.-H. Tung and Q.-Z. Yang, *Angew. Chem., Int. Ed.*, 2013, **52**, 9738; (*b*) P. Wei, J.-X. Zhang, Z. Zhao, Y. Chen, X. He, M. Chen, J. Gong, H.-H. Sung, I. D. Williams, J. W. Y. Lam and B.-Z. Tang, *J. Am. Chem. Soc.*, 2018, **140**, 1966; (*c*) S. J. Wezenberg, C. M. Croisetu, M. C. A. Stuart and B. L. Feringa, *Chem. Sci.*, 2016, **7**, 4341; (*d*) D. Villarón and S. J. Wezenberg, *Angew. Chem., Int. Ed.*, 2020, **59**, 13192; (*e*) J. Luo, K. Song, F.-L. Gu and Q. Miao, *Chem. Sci.*, 2011, **2**, 2029.

5 V. Serreli, C. F. Lee, E. R. Kay and D. A. Leigh, *Nature*, 2007, **445**, 523.

6 D.-H. Qu, Q.-C. Wang and H. Tian, *Angew. Chem., Int. Ed.*, 2005, **44**, 5296.

7 C. C. Price and M. Meister, *J. Am. Chem. Soc.*, 1939, **61**, 1595.

8 D. S. Noyce, D. R. Hartter and F. B. Miles, *J. Am. Chem. Soc.*, 1968, **90**, 4633.

9 M. S. Kharasch, J. V. Mansfield and F. R. Mayo, *J. Am. Chem. Soc.*, 1937, **59**, 1155.

10 (*a*) X. Guo, B. Shao, S. Zhou, I. Aprahamian and Z. Chen, *Chem. Sci.*, 2020, **11**, 3016; (*b*) C. L. Fleming, S. Li, M. Grøtli and J. Andréasson, *J. Am. Chem. Soc.*, 2018, **140**, 14069; (*c*) A. Kerckhoffs and M. J. Langton, *Chem. Sci.*, 2020, **11**, 6325.

11 C. F. Bernasconi and W. J. Boyle, *J. Am. Chem. Soc.*, 1974, **96**, 6070.

12 (*a*) C. Biagini and S. D. Stefano, *Angew. Chem., Int. Ed.*, 2020, **59**, 8344; (*b*) C. Biagini, S. Albano, R. Caruso, L. Mandolini, J. A. Berrocal and S. D. Stefano, *Chem. Sci.*, 2018, **9**, 181.

13 I. Cvrtila, H. Fanlo-Virgós, G. Schaeffer, G. Monreal Santiago and S. Otto, *J. Am. Chem. Soc.*, 2017, **139**, 12459.

14 (*a*) D. Bléger and S. Hecht, *Angew. Chem., Int. Ed.*, 2015, **54**, 11338; (*b*) A. H. Heindl, J. Becker and H. A. Wegner, *Chem. Sci.*, 2019, **10**, 7418; (*c*) G. M. Peters and J. D. Tovar, *J. Am. Chem. Soc.*, 2019, **141**, 3146; (*d*) S. Fredrich, A. Bonasera, V. Valderrey and S. Hecht, *J. Am. Chem. Soc.*, 2018, **140**, 6432; (*e*) N. A. Simeth, A. C. Kneuttinger, R. Sterner and B. König, *Chem. Sci.*, 2017, **8**, 6474; (*f*) D. B. Konrad, G. Savasci, L. Allmendinger, D. Trauner, C. Ochsenfeld and A. M. Ali, *J. Am. Chem. Soc.*, 2020, **142**, 6538; (*g*) Z. Xu, Q. T. Liu, X. Wang, Q. Liu, D. Hean, K. C. Chou and M. O. Wolf, *Chem. Sci.*, 2020, **11**, 2729.

15 (*a*) I. Hnid, D. Frath, F. Lafolet, X. Sun and J. C. Lacroix, *J. Am. Chem. Soc.*, 2020, **142**, 7732; (*b*) J. Yin, A. N. Khalilov, P. Muthupandi, R. Ladd and V. B. Birman, *J. Am. Chem. Soc.*, 2020, **142**, 60; (*c*) M. Herder, M. Utecht, N. Manicke, L. Grubert, M. Pätzel, P. Saalfrank and S. Hecht, *Chem. Sci.*, 2013, **4**, 1028.

16 (*a*) T. Ooi, *Science*, 2011, **331**, 1395; (*b*) N. Mallo, E. D. Foley, H. Iranmanesh, A. D. W. Kennedy, E. T. Luis, J. Ho, J. B. Harper and J. E. Beves, *Chem. Sci.*, 2018, **9**, 8242; (*c*) C. Poloni, M. C. A. Stuart, P. Meulen, W. Szymanski and B. L. Feringa, *Chem. Sci.*, 2015, **6**, 7311.

17 (*a*) J. D. Badjic, V. Balzani, A. Credi, S. Silvi and J. F. Stoddart, *Science*, 2004, **303**, 1845; (*b*) X. Fu, H. Han, D. Zhang, H. Yu, Q. He and D. Zhao, *Chem. Sci.*, 2020, **11**, 5565.

18 A. Martinez, L. Guy and J.-P. Dutasta, *J. Am. Chem. Soc.*, 2010, **132**, 16733.

19 (*a*) S. P. Fletcher, F. Dumur, M. M. Pollard and B. L. Feringa, *Science*, 2005, **310**, 80; (*b*) T. R. Kelly, H. D. Silva and R. A. Silva, *Nature*, 1999, **401**, 150; (*c*) J. T. Foy, D. Rayb and I. Aprahamian, *Chem. Sci.*, 2015, **6**, 209; (*d*) P. C. Knipe, S. Thompson and A. D. Hamilton, *Chem. Sci.*, 2015, **6**, 1630.

20 J. Yao, W. Wu, W. Liang, Y. Feng, D. Zhou, J. J. Chruma, G. Fukuhara, T. Mori, Y. Inoue and C. Yang, *Angew. Chem., Int. Ed.*, 2017, **56**, 6869.

21 C. Xiao, W. Wu, W. Liang, D. Zhou, K. Kanagaraj, G. Cheng, D. Su, Z. Zhong, J. J. Chruma and C. Yang, *Angew. Chem., Int. Ed.*, 2020, **59**, 8094.

22 (*a*) M. M. Lerch, M. J. Hansen, W. A. Velema, W. Szymanski and B. L. Feringa, *Nat. Commun.*, 2016, **7**, 12054; (*b*) D. Roke, C. Stuckhardt, W. Danowski, S. J. Wezenberg and B. L. Feringa, *Angew. Chem., Int. Ed.*, 2018, **57**, 10515; (*c*) E. Fuentes, M. Gerth, J. A. Berrocal, C. Matera, P. Gorostiza, I. K. Voets, S. Pujals and L. Albertazzi, *J. Am. Chem. Soc.*, 2020, **142**, 10069; (*d*) A. Goulet-Hanssens, M. Utecht, D. Mutruc, E. Titov, J. Schwarz, L. Grubert, D. Bleger, P. Saalfrank and S. Hecht, *J. Am. Chem. Soc.*, 2017, **139**, 335.

23 T.-T. Hao, H.-R. Liang, Y.-H. Ou-Yang, C.-Z. Yin, X.-L. Zheng, M.-L. Yuan, R.-X. Li, H.-Y. Fu and H. Chen, *J. Org. Chem.*, 2018, **83**, 4441.

24 M. B. Smith and J. March, *March's Advanced Organic Chemistry: Reactions, Mechanisms, and Structure*, 6th edn, Wiley, New York, USA, 2006.

25 (*a*) J. Bredt, J. Houben and P. Levy, *Ber. Dtsch. Chem. Ges.*, 1902, **35**, 1286; (*b*) F. S. Fawcett, *Chem. Rev.*, 1950, **47**, 219; (*c*) K. B. Wiberg, *Angew. Chem., Int. Ed.*, 1986, **25**, 312; (*d*) Z. Huang, Q. Z. Yang, D. Khvostichenko, T. J. Kucharski, J. Chen and R. Boulatov, *J. Am. Chem. Soc.*, 2009, **131**, 1407; (*e*) R. Siewertsen, H. Neumann, B. Buchheim-Stehn, R. Herges, C. Näther, F. Renth and F. Temps, *J. Am. Chem. Soc.*, 2009, **131**, 15594; (*f*) Q. Li, H. Qian, B. Shao, R. P. Hughes and I. Aprahamian, *J. Am. Chem. Soc.*, 2018, **140**, 11829.

26 A. D. Allen, M. Resenbaum, N. O. L. Seto and T. T. Tidwell, *J. Org. Chem.*, 1982, **47**, 4234.

27 A. K. Chew, T. W. Walker, Z. Shen, B. Demir, L. Witteman, J. Euclide, G. W. Huber, J. A. Dumesic and R. C. Van Lehn, *ACS Catal.*, 2020, **10**, 1679.

28 (*a*) S. M. Landge and I. Aprahamian, *J. Am. Chem. Soc.*, 2009, **131**, 18269; (*b*) X. Su, T. F. Robbins and I. Aprahamian, *Angew. Chem., Int. Ed.*, 2011, **50**, 1841; (*c*) X. Su and I. Aprahamian, *Chem. Soc. Rev.*, 2014, **43**, 1963; (*d*) I. Aprahamian, *Chem. Commun.*, 2017, **53**, 6674.

29 (*a*) Y. Ren, P. H. Svensson and O. Ramström, *Angew. Chem., Int. Ed.*, 2018, **57**, 6256; (*b*) Y. Ren, S. Xie, E. Svensson Grape, A. K. Inge and O. Ramström, *J. Am. Chem. Soc.*, 2018, **140**, 13640.

30 L. A. Tatum, J. T. Foy and I. Aprahamian, *J. Am. Chem. Soc.*, 2014, **136**, 17438.

31 G.-Y. Zhao and T. Wang, *Angew. Chem., Int. Ed.*, 2018, **57**, 6120.

32 (*a*) M.-X. Wang, Y.-M. Chen, Y. Gao, C. Hu, J. Hu, L. Tan and Z. Yang, *ACS Appl. Mater. Interfaces*, 2018, **10**, 26610; (*b*) H. J. Sim, H. Kim, Y. Jang, G. M. Spinks, S. Gambhir, D. L. Officer, G. G. Wallace and S. J. Kim, *ACS Appl. Mater. Interfaces*, 2019, **11**, 46026.

33 (*a*) N. A. Simeth, S. Crespi, M. Fagnoni and B. König, *J. Am. Chem. Soc.*, 2018, **140**, 2940; (*b*) C. E. Weston, R. D. Richardson, P. R. Haycock, A. J. White and M. J. Fuchter, *J. Am. Chem. Soc.*, 2014, **136**, 11878; (*c*) D. Bleger, J. Schwarz, A. M. Brouwer and S. Hecht, *J. Am. Chem. Soc.*, 2012, **134**, 20597; (*d*) H. Qian, Y. Y. Wang, D. S. Guo and I. Aprahamian, *J. Am. Chem. Soc.*, 2017, **139**, 1037; (*e*) L. Pesce, C. Perego, A. B. Grommet, R. Klajn and G. M. Pavan, *J. Am. Chem. Soc.*, 2020, **142**, 9792; (*f*) Q. Li, H. Qian, B. Shao, R. P. Hughes and I. Aprahamian, *J. Am. Chem. Soc.*, 2018, **140**, 11829; (*g*) Z. Chu, Y. Han, T. Bian, S. De, P. Kral and R. Klajn, *J. Am. Chem. Soc.*, 2019, **141**, 1949.

34 (*a*) X. Wei, W. Wu, R. Matsushita, Z. Yan, D. Zhou, J. J. Chruma, M. Nishijima, G. Fukuhara, T. Mori, Y. Inoue and C. Yang, *J. Am. Chem. Soc.*, 2018, **140**, 3959; (*b*) X. Wei, J. Liu, G. J. Xia, J. Deng, P. Sun, J. J. Chruma, W. Wu, C. Yang, Y. G. Wang and Z. Huang, *Nat. Chem.*, 2020, **12**, 551; (*c*) J. Ji, W. Wu, W. Liang, G. Cheng, R. Matsushita, Z. Yan, X. Wei, M. Rao, D. Q. Yuan, G. Fukuhara, T. Mori, Y. Inoue and C. Yang, *J. Am. Chem. Soc.*, 2019, **141**, 9225; (*d*) C. Yang and Y. Inoue, *Chem. Soc. Rev.*, 2014, **43**, 4123.

35 (*a*) B. L. Feringa, R. A. van Delden, N. Koumura and E. M. Geertsema, *Chem. Rev.*, 2000, **100**, 1789; (*b*) Y. Wang and Q. Li, *Adv. Mater.*, 2012, **24**, 1926; (*c*) J. Li, H. K. Bisoyi, S. Lin, J. Guo and Q. Li, *Angew. Chem., Int. Ed.*, 2019, **58**, 16052.